Oil Shale, 2023, Vol. 40, No. 3, pp. 244–259
doi: https://doi.org/10.3176/oil.2023.3.05
ISSN 0208-189X

A case study to improve blasting efficiency by the use of emulsion explosives

Sergei Sabanov[(a)*], Oleg Nikitin[(b)], Abdullah Qureshi[(a)], Zhaudir Dauitbay[(a)]

[(a)] School of Mining and Geosciences, Nazarbayev University, 53 Kabanbay Batyr Ave., Nur-Sultan city, Republic of Kazakhstan
[(b)] Eesti Energia, Enefit Power AS, Estonia

Received 23 January 2023, accepted 21 July 2023, available online 10 September 2023

Abstract. *This work analyses issues associated with the deteriorated blasting efficiency by the use of emulsion explosives in underground oil shale mines that utilise room and pillar mining methods. The problems were connected with the reduction in entry advance, shattering of pillar walls and falling of the roof. The aim of this study is to improve blasting efficiency that can guarantee a sufficient entry advance and secure stable conditions of the pillars and the immediate roof. The improved blasting pattern was successfully tested under in-situ conditions. It was demonstrated that the entry advance and the stability of the immediate roof and pillar walls were significantly enhanced as a result.*

Keywords: *blasting efficiency, emulsion explosives, velocity of detonation, blasting energy distribution, specific charge.*

1. Introduction

Controlled use of explosives is applied to break rocks for excavation in mining, quarrying, and civil engineering. Explosive efficiency relies on the appropriate selection of a blasthole diameter and length, a space, a burden and firing sequences. Based on field tests, Ittner et al. [1] summarised that blast fracture length improved when hole spacing increased. At the same time, variations in burden had a limited influence on blast fracture length. Cunningham and Goetzsche [2] and Ivanova [3] established that drilling deviation influences blasting efficiency and fragmentation. According to Persson et al. [4] it is necessary to study the character, strength, orientation, size and frequency of natural fractures for the purposes of making a statement to the extent of

* Corresponding author: e-mail s*ylvester.ofili@ut.ee*

damage to the remaining rock. Ittner et al. [1] derived that natural fractures can behave as barriers to blast fracture extension where only around 30% of them might intersect open natural fractures. Olsson and Ouchterlony [5] formulated a method that estimates the length of the longest blast fracture with the help of an uncorrected fracture length, modified by correction factors for specific geological, geometrical and initiation conditions:

$$Rc = Rco * Fh * Ft * Fv * Fb, \quad (1)$$

where Rc is the length of the longest blast fracture, Rco is the uncorrelated fracture length, Fh is the correction factor for hole spacing, Ft is the correction factor for spread in initiation time, Fv is the correction factor for wet holes and Fb is the correction factor for rock type and fracturing.

The uncorrected fracture length is calculated based on decoupling ratio charge concentration and velocity of detonation (VOD) [1]. One of the important characteristics of explosives is VOD, which can be defined as the velocity at which the shock wave front travels through a detonated explosive [6]. VOD is an important property to consider when rating an explosive [7]. It has been observed that most manufacturers and utilities companies rely on calculations based on the chemical composition of a bulk explosive to arrive at the VOD value. Tete et al. [7] assumed that such an interpretation can be somewhat inaccurate due to variations in raw material quality and the manufacturing processes followed, and, more importantly, it is still only a theoretical value. Deriving the correct VOD value with appropriate measurement techniques will result in a reduction in the consumption of explosives with optimized results. Explosives with a low velocity of detonation will have a less significant impact on rock fragmentation than those with a high VOD [8, 9].

Emulsion explosives became widely used due to the advantage of the safe transportation of all their components separately to the mine site, while these explosives become active only when the components are mixed and make a blasthole explosive. One of the features, apart from low sensitivity to mechanical impact, is that the density of an explosive emulsion may vary widely, which leads to different VOD. The variation in the emulsion explosive's density causes an equivalent change in energy per unit volume. In addition, emulsion explosives can be easily injected into an offset blasthole while cartridge explosives could stuck midway [10].

The purpose of this study is to improve blasting efficiency that can guarantee a sufficient entry advance and secure stable conditions of the pillars and the immediate roof. The emulsion explosives' velocity of detonation and the relationship between the blast damage radius and the charge concentration have been established by the experimental tests. Modelling of the improved blasting pattern takes into consideration the quality of emulsion explosives, properties of rock, simulation of detonation, distribution of explosive energy, and estimation of the blast damage radius around a blasthole depending on the specific charge. The modelling results were validated by the mine test data.

2. Case study description

The study mine employs large-scale room and pillar mining that produces oil shale via conventional drilling and blasting followed by mucking to conveyors, which transport oil shale to a beneficiation plant located on surface. The size of the columns and rooms depends on the quality of the miners' work, but also on geological factors [11]. The roof support is provided by drilling a 42 mm diameter hole and installing a 16 mm diameter rebar with a face plate and shell anchor with a bolting pattern of 1.5 m × 1.5 m (regular conditions) or 1.2 m × 1.2 m (complex conditions) [12]. The local oil shale is composed of stratified sedimentary rock rich in organic matter (15–46% kerogen, 26–57% carbonates, and 18–42% clastic materials). Within the tectonic dislocation zones the karst clay content is about 10–15%. Fractured zones are typically abundant in water and unstable. The rock in the fractured zones is dolomitized and contains some calcite and pyrite veins, sometimes with marcasite, galena, sphalerite and barite [13]. The oil shale uniaxial compressive strength (UCS) is measured at 18–40 MPa, and that for limestone is measured at 65–82 MPa (Table 1). The volume density of these rocks varies from 1.2 to 1.7 t/m^3 and from 2.1 to 2.5 t/m^3, respectively. Young's modulus for layer C is E ~ 7.1 GPa and σr ~ 2.5 MPa [14, 15].

Table 1. Oil shale and embedded limestone data

Layer index	Thickness, m	UCS, MPa	Density, t/m^3
F3	0.37	25	1.73
F2/F3	0.11	67	2.12
F2	0.17	24	1.72
F1/F2	0.18	65	2.10
F1	0.20	26	1.51
F	0.42	24	1.51
E	0.58	18	1.28
D/E	0.07	67	2.10
D	0.06	29	1.59
C/D	0.29	82	2.45
C	0.41	26	1.38
B/C	0.12	75	2.10
B	0.38	40	1.22
A1/B	0.18	65	2.25
A1	0.09	26	1.42
A/A1	0.06	32	2.10
A	0.12	32	1.37

The mine uses an underground bulk emulsion explosives system through which waterproof emulsion explosives are injected by charging equipment into 38-mm-diameter blastholes at a depth of 4.0 m. These waterproof emulsion explosives were specially designed for underground blasting operations for oil shale mines, which pose dust explosion hazards. Technical properties of the emulsion explosives are presented in Table 2.

Table 2. Technical parameters of explosives

Parameter	Value
Blasting energy, kJ/kg	2900–2950
Evolving gas volume, l/kg	900–990
Detonation velocity, km/s	3.80–4.50
Density, g/cm^3	0.80–1.00
Oxygen balance	–0.90–0.00

A typical cut is employed by drilling six or nine cut holes into the central part of the face. Cut holes are 4.0 m in depth and 280 mm in diameter. Working face dimensions are roughly 7 m wide and 3.8 m high. The blasting period of millisecond detonators (250 ms), with a detonation sequence of 1 to 18, is 4.5 seconds.

3. Materials and methods

3.1. Blasting modelling

After explosive detonation, a blasthole is filled with gaseous detonation products at very high pressure and temperature. This pressure is immediately exerted onto the walls of the blasthole (Fig. 4), generating radial compressive stress levels much stronger than the strength of rock in the thin zone around the blasthole, from which the rock is yielded and extensively broken or crushed through granular cracking, micro-cracking, differential rock particle and matrix compression and other forms of plastic deformation [16]. Cracking radius is of prime concern and should be very carefully controlled [17].

Thorne et al. [18] described a finite element model based on the constitutive damage concept developed by Grady and Kipp [19], Taylor et al. [20] and Kuszmaul [21], in which case fragmentation is achieved through the continual accumulation of damage in an isotropic material with microcracks [22]. The study recognises the gradual degradation of material strength with time and its incorporation of microcracks, which can interact and grow into macrocracks [17].

Grady and Kipp [19] used the fracture model, which has been incorporated into one- and two-dimensional stress-wave computer codes and has been used to evaluate blasting geometries and stress-pulse tailoring for the in-situ rubblization of oil shale. An et al. [23] retrieved results that can predict a small average fragment size close to a borehole grading rapidly to larger fragment sizes with increasing range as a consequence of the decreasing effective rate of strain at which the material is carried into tension with increasing distance from the borehole.

The model for the estimation of the extent of crushing around a blasthole proposed by Kanchbolta et al. [24] estimates the radius of crushing as a function of the borehole radius, the detonation pressure level and the unconfined compressive strength. This is expressed by the following relationship:

$$r_c = r_o\sqrt{\frac{Pd}{\sigma c}}, \tag{2}$$

where r_o is the borehole radius, mm; Pd is the detonation pressure level, Pa; and σc is the unconfined compressive strength of the rock, Pa.

Esen at al. [25] carried out experiments to have data for using this model in order to produce accurate results, because the detonation pressure calculated is for ideal detonation behaviour. Ideal detonation assumes that the flow is one-dimensional [26], the plane detonation front is a jump discontinuity, a shock in which a chemical reaction is assumed to be completed and the jump discontinuity is steady [19].

According to Cooper [27], an explosive's VOD is widely used to estimate its detonation pressure level and explosive shock energy contained in the substance material. The detonation pressure level (Pd) of an explosive is expressed by the unreacted explosive density and VOD by the following formula [22, 28]:

$$Pd = \frac{\rho e\, Cd^2}{\gamma + 1}, \tag{3}$$

where Pd is the detonation pressure level, GPa; ρe is the explosive density, g/cm^3; Cd is the VOD, m/s; and γ is the ratio of the specific heat of detonation product gases, $\gamma \sim 3$.

Cunningham [29] stated that γ may be approximately 2.6 for Ammonium Nitrate Fuel Oil (ANFO) to 3.2 for emulsion. A reduction in VOD will produce a decrease in both the Pd value and the shock energy level of the explosive [7].

Considering Equations (2) and (3) for our case, the blast damage radius (Rd) for the roof, wall and floor, and blastholes can be estimated using the following equation:

$$Rd = 1.65 r_o \sqrt{\frac{\rho e\, C^2}{4\sigma c}}. \tag{4}$$

This blast damage radius is recommended to use for checking safe distances from blastholes to the final contours of the designed roof, wall and floor (Fig. 1). Figure 1 also presents a schematic illustration of the crushing zone around the blasthole, the fragment formation zones, and the blast damage radius (a red circle around the pink zone). If the blast damage radius intersects the designed final contours development, it might create unstable mining conditions after blasting. To avoid this, the blasthole arrangement should be re-designed considering the blast damage radius, or the charge concentration should be changed. The factor 1.65 for the blast damage radius in Equation (4) was established during the experimental tests and validated by the blasting pattern modelling results.

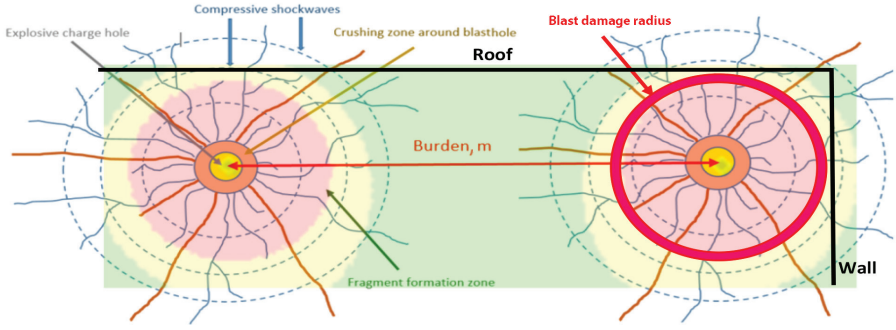

Fig. 1. Schematic illustration of the crushing, fracture and fragment formation zones and the blast damage radius.

The blast damage radius calculated with the help of Equation 4 (Fig. 1) is related to the charge specific volume around the blast, which is called the Kleine Field. This field is the basis of an isosurfacing mechanism in the 3D ring [30]. According to Kleine et al. [31], the traditional specific charge calculation was extended by considering a small infinitesimal segment of charge and writing the equation for the resulting explosive concentration at point P for a sphere centred at the charge segment (Fig. 2); the general form of the equation is as follows:

$$P = \int_{L1}^{L2} \frac{1000\,\rho_e\,\pi(\frac{D}{2})^2}{\rho_r \frac{4}{3}\pi\,(h^2+l^2)^{\frac{2}{3}}}\,dl. \tag{5}$$

The explosive concentration (Fig. 2) at any point in 3D is determined by solving the appropriate integrated form of the equation for each explosive charge and summing the values obtained by Kleine et al. [32].

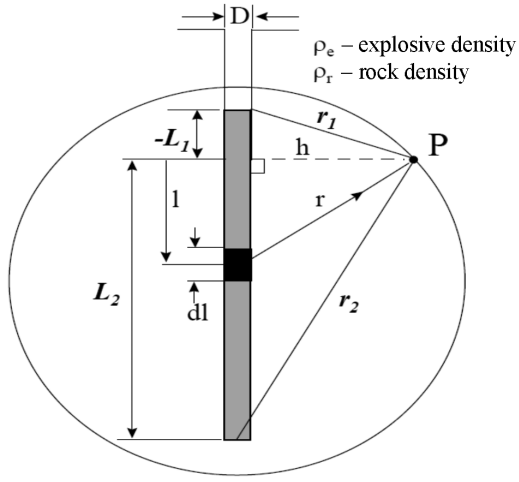

Fig. 2. Geometry for the solution to the Kleine Field [32].

Equation (5) can be integrated and rewritten according to Kleine et al. [32] as follows:

$$P = 187.5 \frac{\rho_e}{\rho_r} D^2 \frac{1}{h^2} \left(\frac{L_2}{r_2} - \frac{L_1}{r_1} \right). \quad (6)$$

The simulation of detonation and explosive energy distribution, which is used for modelling a blasting pattern, considers the blastholes arrangement, explosive strength, rock density and strength, as well as charging structure and detonation timing. The simulation utilised JKSimBlast software, the 4D explosive energy distribution considering detonation timing as the fourth dimension. The JKSimBlast 4D model integrates a function of the time a deck detonates and a rock mass specific factor, where a timing simulation is carried out first. Thus, the simulation of the blast detonation sequence sets up the time step of a simulation and runs the Monte Carlo simulation. The analysis checks the degree of burden relief of each deck at the moment of detonation. For the Monte Carlo detonation simulation the program calculates the number of times a deck is a success or a failure based on a criteria defined by three items:

- the number of other charges detonating within the proximity, distance (m) and at least several milliseconds (ms) before the current deck;
- the proximity distance (m) generally defined by the largest distance between the holes in a pattern;
- the time required for the rock to move to be associated with the burden movement time of the rock mass being blasted.

Summing up the methodology, the specific charge can control the blast damage radius, which will rely on the modelled factor used for estimation of the extent of crushing around a blasthole.

3.2. Measurement techniques

According to Tete at al. [7], velocity of detonation is an important measure that determines the parameters of the explosive material, while the explosive's performance invariably depends on VOD. Using appropriate VOD measurement techniques will diminish the consumption of explosives. VOD measurements can be performed by the point-to-point fibre optic method that uses optical fibres which can detect and transmit a light signal traveling with the detonation wave front. This means that the first cable signals the start, while the second cable arranged at a predetermined fixed interval stops the timer. The fixed interval between the two cable signals divided by the timed period is the VOD value [7].

4. Results and discussion

4.1. Velocity of detonation measurement

Velocity of detonation was measured using the fibre optic method to evaluate the performance of emulsion explosives. The method uses optical fibres for detecting and transmitting a light signal accompanying a detonation wave front in the borehole. Emulsion explosives from two different batches ("old" and "fresh") were tested. Old emulsion explosives were stored in the underground mine for 45 days, while fresh emulsion explosives had recently been delivered from an explosives plant. Six blastholes of 38 mm in diameter were drilled at a depth of 4 m within the mine study area. A VOD measurement tool composed of a steel stick of 3500 mm in length and 4 mm in diameter was placed into each blasthole. Two simplex plastic optical fibre cables were attached along this steel stick. 3.5 kg of emulsion explosives was injected into each blasthole. The Explomet-FO-2000 measuring device measured the time intervals in microseconds between the illumination of two consecutive probes and calculated VOD in meters per second. The old and fresh emulsion explosives were charged. The results of VOD measurements are presented in Figure 3.

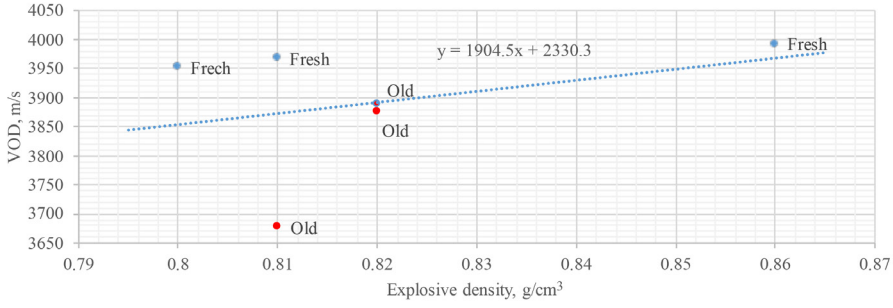

Fig. 3. Velocity of detonation measurement results.

The initial temperature of the old emulsion explosives was measured to be 13.4 °C and that of the fresh emulsion explosives, 25 °C. The temperature of the surrounding rocks was measured to be 9.4 °C and of the air temperature, 9.9 °C. VOD values recorded from the mine area ranged from 3677 to 3867 m/s for the old emulsion explosives and from 3957 to 3992 m/s for the fresh ones. These results are generally consistent with the VOD given by the manufacturer whose range is based on minimum unconfined and calculated ideal (Table 2). However, the company uses only freshly prepared explosives for further blasting operations and never those from the underground mine storage. As a result, the nominal VOD of 3900 m/s at a density of 0.82 g/cm^3 has been accepted for these emulsion explosives at a blasthole diameter of 38 mm. These VOD field test results were used for modelling the improved blasting pattern.

4.2. Improvement of the blasting pattern

The originally designed blasting pattern of 75.0 kg exhibited in some cases a diminished entry advance, which was just over 3.3 m and therefore had an average weight-to-volume ratio of 0.85 kg/m^3. For several reasons this blasting pattern was not able to guarantee the entry advance of 4.0 m. Considering this, the blast simulation was performed with the help of JKSimBlast software, which allowed quantifying blasting energy range, showing its distribution within the blasting pattern. The simulation results presented in Figure 4 show that the high blast energy concentration (red zones in the figure) at the F3 layer holes intersect with the roof. This extensive blasting energy influenced the immediate roof stability (roof exfoliation and fall), which actually took place at the tested mining areas. The blue zones at the A layer holes demonstrated insufficient blasting energy that was unable to produce a flat level floor (Fig. 4). These simulation results were compared with the field test data and were used to improve the originally designed blasting pattern.

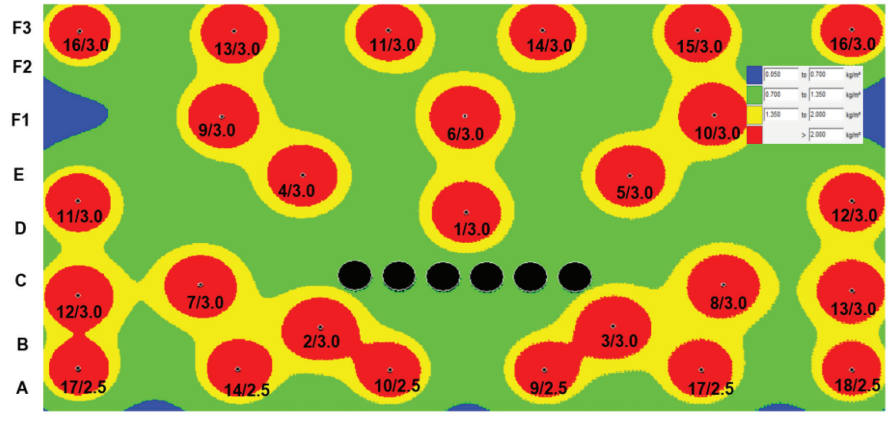

Fig. 4. Explosive energy distribution at the original blasting pattern of 75 kg.

Based on the simulation results and collected field test data, it has been proposed to improve the blasting pattern by relocating charge distributions according to the highlighted issues with the roof, floor and entry advance. Detonation sequence was not changed. As a result, the improved blasting pattern of 75.0 kg (I) has decreased the charge concentration of the F3 layer by 2.2 kg to secure the roof stability and that of the C layer to secure the pillar walls. At the same time, the improved blasting pattern has an increased charge concentration of 0.8 kg on average for layers F1, D and B to enhance the entry advance, and 1.4 kg on average for layer A to guarantee the flat level floor (Table 3).

Table 3. Comparison of blasting patterns of 75 kg and 75 kg (I)

Layer index	Layer UCS, MPa	Pattern 75, kg	Pattern 75 (I), kg	Difference, kg
F_3	23	18	15.8	–2.2
F_1	19	9	9.2	0.2
D	30	15	15.4	0.4
C	26	12	11.6	–0.4
B	40	6	6.2	0.2
A	32	15	16.8	1.8
Total		75	75	0

For the improved blasting pattern of 75 kg (I) the Monte Carlo simulation was run to validate the blast detonation sequence by checking the degree of burden of each hole at the instant of detonation. For the Monte Carlo detonation simulation the JKSimBlast software program calculated the number of times a hole is either a success or a failure based on criteria defined by the number of other charges which detonate within a distance (1.33 m) and at least several milliseconds (ms) before the current hole. The output shows green coloured holes, which have a 100% probability success in this blast within the proximity distance of 1.33 m that corresponds to the holes burden relief of the improved blasting pattern (Fig. 5). The proximity distance is generally defined by the largest distance between holes in a pattern. Time contours are also shown in Figure 5. The time required (ms) for the rock to move is associated with the burden movement time of the rock mass being blasted.

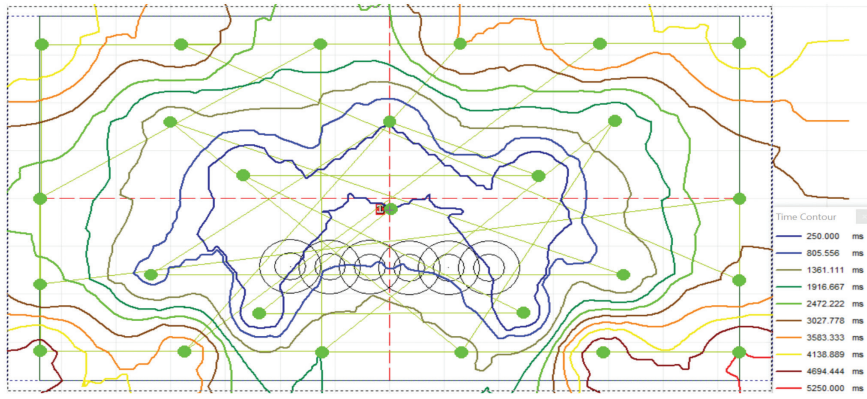

Fig. 5. Time contours in the detonation sequence simulation for the optimised blasting pattern of 75 kg (I).

The simulation results (Fig. 6) demonstrate a better explosive energy distribution for the improved blasting pattern of 75 kg (I) and also show that red zones with a high energy concentration do not intersect with the roof and wall.

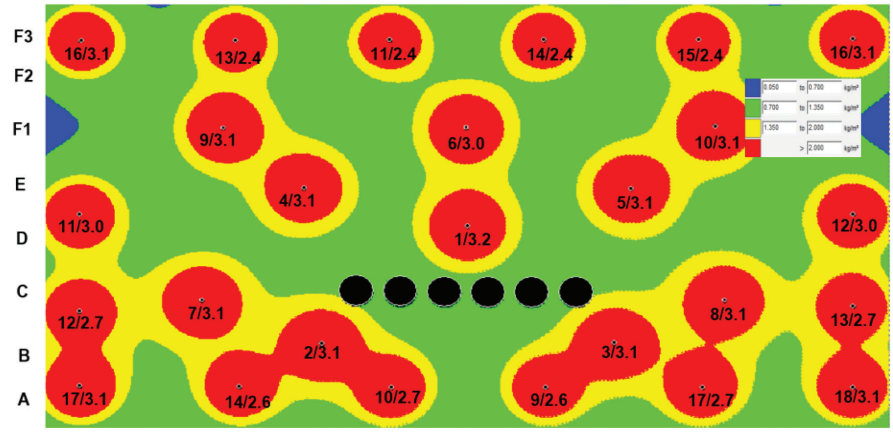

Fig. 6. Explosive energy distribution for the improved blasting pattern of 75 kg (I).

The simulation results were validated by the field test data obtained, proving stable conditions for the immediate roof and the existence of the flat floor. Thus, the improved blasting pattern of 75 kg (I) increased the entry advance to 4.0 m and provided a higher average weight-to-volume ratio of 0.70 kg/m^3 compared to the 0.85 kg/m^3 of the originally designed blasting pattern.

Based on the field test data collected, relationships between the blast damage radius (high blasting energy concentration) and the specific charge for roof, floor and wall holes have been derived (Fig. 7).

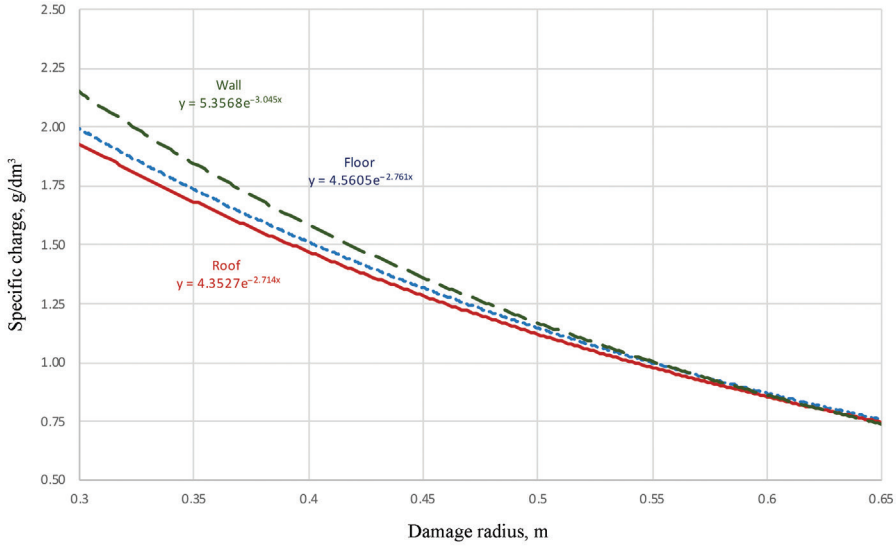

Fig. 7. Relationships between the specific charge and the damage radius.

These relationships can be combined with Equation (4), which calculates the damage radius (Rd) for estimation of the specific charge (SC). For example, SC for the immediate roof holes is estimated as follows:

$$SC = 4.4e^{-2.7Rd}. \tag{7}$$

Thus, for the improved blasting pattern where the holes are located at 0.3 m away, for example, from the immediate roof final contour, the specific charge within this damage radius (0.3 m) should not exceed 1.9 g/dm^3 for the roof holes. Similar calculations can be performed using the exponential correlations from Figure 7 for the floor and wall holes. These relationships (Fig. 7) of the specific charge to the blast damage radius can be used for estimation of the extent of the crushing zones around a blasthole.

As a result, the improved blasting pattern of 75 kg (I), taking into account interrelations between emulsion explosives parameters, rock types and the blast damage radius from the specific charge, was worked out. The improved blasting pattern was successfully tested under in-situ conditions, demonstrating that the blasting efficiency considering the sufficient entry advance with secured roof, floor, and pillar wall stability was significantly enhanced.

5. Conclusions

This case study analysed issues associated with deteriorated blasting efficiency and produced the improved blasting pattern that is able to guarantee appropriate entry advance and can provide stable conditions of the pillars and the immediate roof. Modelling of the improved blasting pattern considered the quality of emulsion explosives, rock properties, simulation of detonation and explosive energy distribution, and estimation of the blast damage radius around a blasthole depending on the specific charge.

The quality of emulsion explosives was analysed based on the velocity of detonation values, which were derived from the mine tests and were used in the modelling of the improved blasting pattern. The nominal VOD of 3900 m/s at a density of 0.82 g/cm^3 has been accepted for these emulsion explosives at a blasthole diameter of 38 mm.

By the experimental tests the relationships between the blast damage radius and the specific charge for roof, floor and wall blastholes have been derived. These relationships can be used for estimation of the extent of crushing zones around a blasthole, which can be controlled by the emulsion explosives charge concentration (the specific charge). The blast damage radius is recommended to use for checking safe distances from blastholes to final contours of the designed developments. As a result, the improved blasting pattern has a decreased charge concentration in the immediate roof and some of the wall central holes and an increased charge concentration in other blastholes. As a consequence, the improved blasting pattern has a higher weight-to-volume ratio (0.70 kg/m^3) compared to the originally designed blasting pattern (0.85 kg/m^3).

The improved blasting pattern was successfully tested under in-situ conditions. It was demonstrated that the blasting efficiency in terms of the sufficient entry advance and secure stable conditions of the immediate roof and pillars walls was significantly enhanced. The results of this study can be applied to any mine using room-and-pillar mining methods under sedimentary rock geological conditions.

Acknowledgments

This study was supported by Nazarbayev University Grant Programs ”Collaborative Research Project #091019CRP2104” and ”Faculty Development Competitive Research Grant #0122022FD4128”.

The publication costs of this article were partially covered by the Estonian Academy of Sciences.

REFERENCES

1. Ittner, H, Olsson, M., Johansson, D., Schunnesson, H. Multivariate evaluation of blast damage from emulsion explosives in tunnels excavated in crystalline rock. *Tunn. Undergr. Space Technol.*, 2019, **85,** 331–339.
2. Cunningham, C. V. B., Goetzsche, A. F. The specification of blast damage limitations in tunnelling contracts. *Tunn. Undergr. Space Technol*., 1990, **5**(3), 193–198.
3. Ivanova, R. *Investigation on Fragmentation by Blasting*: *The influence of distorted blasthole patterns on fragmentation, roughness of the remaining bench face and blast damage behind it in model scale blasting.* PhD thesis. Montanuniversitaet Leoben, Austria, 2015.
4. Persson, P.-A., Holmberg, R., Lee, J. *Rock Blasting and Explosives Engineering*. CRC Press, Florida, USA, 1993, 101, 106, 107.
5. Olsson, M., Ouchterlony, F. *New Formula for Blast Induced Damage in the Remaining Rock*. Swedish Rock Engineering Research, SveBeFo Rapport 65, 2003 (in Swedish).
6. Mertuszka, P., Cenian, B., Kramarczyk, B., Pytel, W. Influence of explosive charge diameter on the detonation velocity based on emulinit 7L and 8L bulk emulsion explosives. *Cent. Eur. J. Energetic Mater.*, 2018, **15**(2), 351–363.
7. Tete, A. D., Deshmukh, A. Y., Yerpude, R. R. Velocity of detonation (VOD) measurement techniques practical approach. *Int. J. Eng. Technol.*, 2013, **2**(3), 259265.
8. Chiappetta, R. F. Blast monitoring instrumentation and analysis techniques, with an emphasis on field application. *Fragblast Int. J. Blasting Fragm.*, 1998, **2**(1), 79–122.
9. Heit, A. *An Investigation into the Parameters that Affect the Swell Factor Used in Volume and Design Calculations at Callide Open Cut Coal Mine*. PhD thesis. University of Southern Queensland, 2011.
10. Maranda, A., Paszula, J. M., Drobysz, B. Research on detonation parameters of low density emulsion explosives modified by microballoons. *CHEMIK*, 2014, **68**(1), 17–22.
11. Reinsalu, E., Lüütre, E., Põldema, T., Väli, E. Long-term stability of pillars in an underground oil shale mine. *Oil Shale*, 2022, **39**(2), 142–149.
12. Sabanov, S., Pastarus, J.-R., Nikitin, O., Väli, E. Risk assessment of seismic impact on the roof and pillars stability in Estonian underground. *Estonian Journal of Engineering*, 2008, **14**(4), 325–333.
13. Sokman, K., Kattai, V., Vaher, R., Systra, Y. J. Influence of tectonic dislocations on oil shale mining in the Estonia deposit. *Oil Shale*, 2008, **25**(2S), 175–187.
14. Sabanov, S. Comparison of unconfined compressive strengths and acoustic emissions of Estonian oil shale and brittle rocks. *Oil Shale*, 2018, **35**(1), 26–38.
15. Sabanov, S., Madani, N., Mukhamedyarova, Z., Tussupbekov, Y. A risk analysis method for estimation of financial benefits of the existing mine ventilation system. *Mining Metall. Explor.*, 2020, **37**, 1137–1149. https://doi.org/10.1007/s42461-020-00232-7

16. Whittaker, B. N., Singh, R. N., Sun, G. *Rock Fracture Mechanics: Principles, Design and Applications*. Elsevier, Amsterdam, 1992.
17. Iverson, S. R., Hustrulid, W. A., Johnson, J. C. *A New Perimeter Control Blast Design Concept for Underground Metal/Nonmetal Drifting Applications*. DHHS (NIOSH) RI 9691, Report of Investigations/2013. Pittsburgh, PA * Spokane, WA, 2013.
18. Thorne, B. J., Hommert, P. J., Brown, B. Experimental and computational investigation of the fundamental mechanisms of cratering. In: *The Third International Symposium on Rock Fragmentation by Blasting*, Brisbane (Australia), 26–31 August 1990. Fragblast'90, 1990, 117–212.
19. Grady, D. E., Kipp, M. E. Continuum modelling of explosive fracture in oil shale. *Int. J. Rock Mech. Min. Sci. Geomech. Abstr.*, 1980, **17**(3), 147–157.
20. Taylor, L. M., Chen, E.-P., Kuszmaul, J. S. Microcrack-induced damage accumulation in brittle rock under dynamic loading. *Comput. Methods Appl. Mech. Eng.*, 1986, **55**(3), 301–320.
21. Kuszmaul, J. S. A new constitutive model for fragmentation of rock under dynamic loading. In: *Second International Symposium on Rock Fragmentation by Blasting*, Keystone, CO, USA, 23–26 August 1987. Albuquerque, NM (USA), Sandia National Labs, 1987.
22. Kabwe, E. Velocity of detonation measurement and fragmentation analysis to evaluate blasting efficacy. *J. Rock Mech. Geotech. Eng.*, 2018, **10**(3), 523–533.
23. An, H. M., Liu, H. Y., Han, H., Zheng, X., Wang, X. G. Hybrid finite-discrete element modelling of dynamic fracture and resultant fragment casting and muck-piling by rock blast. *Comput. Geotech.*, 2017, **81**, 322–345.
24. Kanchibotla, S. S., Valery, W., Morrell, S. Modelling fines in blast fragmentation and its impact on crushing and grinding. In: *Proceedings of Explo'99: A Conference on Rock Breaking*, 7–11 November 1999, Kalgoorlie, Australia. The Australasian Institute of Mining and Metallurgy, 1999, 137–144.
25. Esen, S., Onederra, I., Bilgin, H. A. Modelling the size of the crushed zone around a blasthole. *Int. J. Rock Mech. Min. Sci.*, 2003, **40**(4), 485–495.
26. Fickett, W., Davis, W. C. *Detonation*. University of California Press, Berkeley, 1979, 16, 54.
27. Cooper, P. W. Acceleration, formation, and flight of fragments. In: *Explosives Engineering*. Wiley-VCH, 1996, 385–394.
28. Yang, J. H., Yao, C., Jiang, Q. H., Lu, W. B., Jiang, S. H. 2D numerical analysis of rock damage induced by dynamic in-situ stress redistribution and blast loading in underground blasting excavation. *Tunn. Undergr. Space Technol.,* 2017*,* **70**, 221–232.
29. Cunningham, C. V. B. The Kuz-Ram model for prediction of fragmentation from blasting. In: *Proceedings of the First International Symposium on Rock Fragmentation by Blasting* (Holmberg, R., Rustan, A, eds.), August 23–26, 1983, Lulea, Sweden, **2**, 439–453.
30. Kleine, T. *A Mathematical Model of Rock Breakage by Blasting*. PhD thesis. The University of Queensland, Australia, 1988.

31. Kleine, T., Cocker, A., Kavetsky, A. The development and implementation of a three dimensional model of blast fragmentation and damage. In: *Proceedings of the Third International Symposium of Rock Fragmentation by Blasting*, Brisbane (Australia), 26–31 August 1990. The Australasian Institute of Mining and Metallurgy, Brisbane, Australia, 181–187.
32. Kleine, T., Townson, P., Riihioja, K. Assessment and computer automated blast design. In: *XXIV International Symposium on the Application of Computers and Operations Research in the Mineral Industries* (Elbrond, J., Tang, X., eds.), Montreal, Canada, 31 Oct.–3 Nov. 1993, **3**, 351–360.